

1. Introduction

This report consists of three tasks, the Task 1 rearranged the grey-box method published by Gori to calculate the heating and cooling demand for the entire building system (GORI, 2017). The equivalent circuit and linear equation are presented, key assumptions made are discussed. The energy consumption and weeks with largest loads difference between lightweight and heavyweight building are performed. The result is discussed with evident facts. Sensitivity analysis, employing both global and local analysis, is conducted for key parameters. The limitations and further works are highlighted.

2. Task 1: lumped capacitance model

The simple dynamic grey-box method (1 thermal mass) incorporating with the solar radiation will be illustrated. This work is not only restricted to calculating the heat flow through one opaque element but emphasise on building a complete system equation to predict the heating and cooling loads requirement for a given condition.

2.1. Equivalent circuit

Concisely, the theory behind calculating the heating and cooling demand is solving the node balance equation. Provided that internal temperature profile from HOBOS, all heat energy flowing in or out of the internal air are combined, equaling to the thermal capacitance of the air. It is assumed that any heat flow entering into the internal air is positive which should be strictly followed for consistency. The temperature difference is the initial subtracts the destination. The overall node balance equation is:

$$\dot{Q}_{HVAC} + \dot{Q}_{solar} + \dot{Q}_{inf.} + \dot{Q}_{vent.} - \dot{Q}_{Win.} - \dot{Q}_{WS} - \dot{Q}_{WW} - \dot{Q}_{WN} - \dot{Q}_{WE} - \dot{Q}_R = \frac{d\dot{Q}}{dt} = C_{air} \frac{dT_{air}}{dt}$$

The total solar radiation through windows is:

$$\dot{Q}_{solar} = gI_{ws}A_{window}$$

Infiltration is assumed to enter the internal air. The temperature difference is external temperature (initial) minus internal temperature (destination).

$$\dot{Q}_{inf.} = \rho_{air}C_{p_{air}}\dot{n}_{inf}V(T_e - T_i)$$

Following the same fashion, the ventilation:

$$\dot{Q}_{vent.} = \rho_{air}C_{p_{air}}\dot{n}_{vent}V(T_e - T_i)$$

In terms of transmission heat transfer, the energy through building fabrics is composed of the window, wall and roof losses. The floor is considered as adiabatic condition and excluded. No heat exchange happening between the floor and soil is rarely true unless an extremely thick insulation is used. This assumption will compromise the overall accuracy of the model.

The heat transfer through windows is shown:

$$\dot{Q}_{win.} = \frac{T_i - T_e}{R_{win.}}A_{win.}$$

It is worth mentioning that the temperature difference for four walls and roof is between the internal air temperature and the thermal mass temperature. The latter one dealing with the dynamic temperature variations at thermal mass is directly adopted from Gori (2017). Furthermore, it is assumed that the first resistance R_1 has accounted for the internal thermal resistance R_{si} .

$$T_c^P = \frac{\frac{T_{int}^P + T_{int}^{P-1}}{R_1} + \left(\frac{2}{\tau}C_1 - \frac{1}{R_1} - \frac{1}{R_2 + R_3}\right)T_c^{P-1} + \frac{T_{ext}^P + T_{ext}^{P-1}}{R_2 + R_3} + \alpha \frac{R_3}{R_2 + R_3}(I_{Sun}^P - I_{Sun}^{P-1})}{\frac{2}{\tau}C_1 + \frac{1}{R_1} + \frac{1}{R_2 + R_3}}$$

$$\dot{Q}_{WS} = \frac{T_i - T_{c,WS}}{R_{1,WS}} A_{WS}$$

$$\dot{Q}_{WW} = \frac{T_i - T_{c,WW}}{R_{1,WW}} A_{WW}$$

$$\dot{Q}_{WN} = \frac{T_i - T_{c,WN}}{R_{1,WN}} A_{WN}$$

$$\dot{Q}_{WE} = \frac{T_i - T_{c,WE}}{R_{1,WE}} A_{WE}$$

$$\dot{Q}_R = \frac{T_i - T_{c,R}}{R_{1,R}} A_R$$

By substitution, the equation can be written as:

$$\begin{aligned} \frac{d\dot{Q}}{dt} = C_{air} \frac{dT_{air}}{dt} &= \dot{Q}_{HVAC} + gI_{ws}A_{win.} + \rho_{air}C_{pair}\dot{n}_{inf}V(T_e - T_i) + \rho_{air}C_{pair}\dot{n}_{vent}V(T_e - T_i) - \frac{T_i - T_e}{R_{win.}}A_{win.} \\ &\quad - \frac{T_i - T_{c,WS}}{R_{1,WS}}A_{WS} - \frac{T_i - T_{c,WW}}{R_{1,WW}}A_{WW} - \frac{T_i - T_{c,WN}}{R_{1,WN}}A_{WN} - \frac{T_i - T_{c,WE}}{R_{1,WE}}A_{WE} - \frac{T_i - T_{c,R}}{R_{1,R}}A_R \end{aligned}$$

Additionally, the obtained linear differential equation will be transformed into an approximated discrete system with the aid of sampling transform. Gori (2017) found that the bilinear transformation is strongly encouraged due to the considerably small approximation errors. The differential equation become:

$$\begin{aligned} \frac{2}{\tau} C_{air} (T_i^P - T_i^{P-1}) &= \left(\dot{Q}_{HVAC}^P + gI_{ws}^P A_{win.} + \rho_{air}C_{pair}\dot{n}_{inf}V(T_e^P - T_i^P) + \rho_{air}C_{pair}\dot{n}_{vent}V(T_e^P - T_i^P) - \frac{T_i^P - T_e^P}{R_{win.}}A_{win.} \right. \\ &\quad - \frac{T_i^P - T_{c,WS}}{R_{1,WS}}A_{WS} - \frac{T_i^P - T_{c,WW}}{R_{1,WW}}A_{WW} - \frac{T_i^P - T_{c,WN}}{R_{1,WN}}A_{WN} - \frac{T_i^P - T_{c,WE}}{R_{1,WE}}A_{WE} - \frac{T_i^P - T_{c,R}}{R_{1,R}}A_R \Big) \\ &\quad + \left(\dot{Q}_{HVAC}^{P-1} + gI_{ws}^{P-1} A_{win.} + \rho_{air}C_{pair}\dot{n}_{inf}V(T_e^{P-1} - T_i^{P-1}) + \rho_{air}C_{pair}\dot{n}_{vent}V(T_e^{P-1} - T_i^{P-1}) \right. \\ &\quad - \frac{T_i^{P-1} - T_e^{P-1}}{R_{win.}}A_{win.} - \frac{T_i^{P-1} - T_{c,WS}}{R_{1,WS}}A_{WS} - \frac{T_i^{P-1} - T_{c,WW}}{R_{1,WW}}A_{WW} - \frac{T_i^{P-1} - T_{c,WN}}{R_{1,WN}}A_{WN} \\ &\quad \left. - \frac{T_i^{P-1} - T_{c,WE}}{R_{1,WE}}A_{WE} - \frac{T_i^{P-1} - T_{c,R}}{R_{1,R}}A_R \right) \end{aligned}$$

Hence the linear equation for HVAC is rewritten as:

$$\begin{aligned} \dot{Q}_{HVAC}^P &= \frac{2}{\tau} C_{air} (T_i^P - T_i^{P-1}) \\ &\quad - \left(\dot{Q}_{HVAC}^{P-1} + gI_{ws}^{P-1} A_{win.} + \rho_{air}C_{pair}\dot{n}_{inf}V(T_e^{P-1} - T_i^{P-1}) + \rho_{air}C_{pair}\dot{n}_{vent}V(T_e^{P-1} - T_i^{P-1}) \right. \\ &\quad - \frac{T_i^{P-1} - T_e^{P-1}}{R_{win.}}A_{win.} - \frac{T_i^{P-1} - T_{c,WS}}{R_{1,WS}}A_{WS} - \frac{T_i^{P-1} - T_{c,WW}}{R_{1,WW}}A_{WW} - \frac{T_i^{P-1} - T_{c,WN}}{R_{1,WN}}A_{WN} \\ &\quad \left. - \frac{T_i^{P-1} - T_{c,WE}}{R_{1,WE}}A_{WE} - \frac{T_i^{P-1} - T_{c,R}}{R_{1,R}}A_R \right) \\ &\quad - \left(gI_{ws}^P A_{win.} + \rho_{air}C_{pair}\dot{n}_{inf}V(T_e^P - T_i^P) + \rho_{air}C_{pair}\dot{n}_{vent}V(T_e^P - T_i^P) - \frac{T_i^P - T_e^P}{R_{win.}}A_{win.} \right. \\ &\quad \left. - \frac{T_i^P - T_{c,WS}}{R_{1,WS}}A_{WS} - \frac{T_i^P - T_{c,WW}}{R_{1,WW}}A_{WW} - \frac{T_i^P - T_{c,WN}}{R_{1,WN}}A_{WN} - \frac{T_i^P - T_{c,WE}}{R_{1,WE}}A_{WE} - \frac{T_i^P - T_{c,R}}{R_{1,R}}A_R \right) \end{aligned}$$

The resulting equivalent circuit is shown in Fig 1.

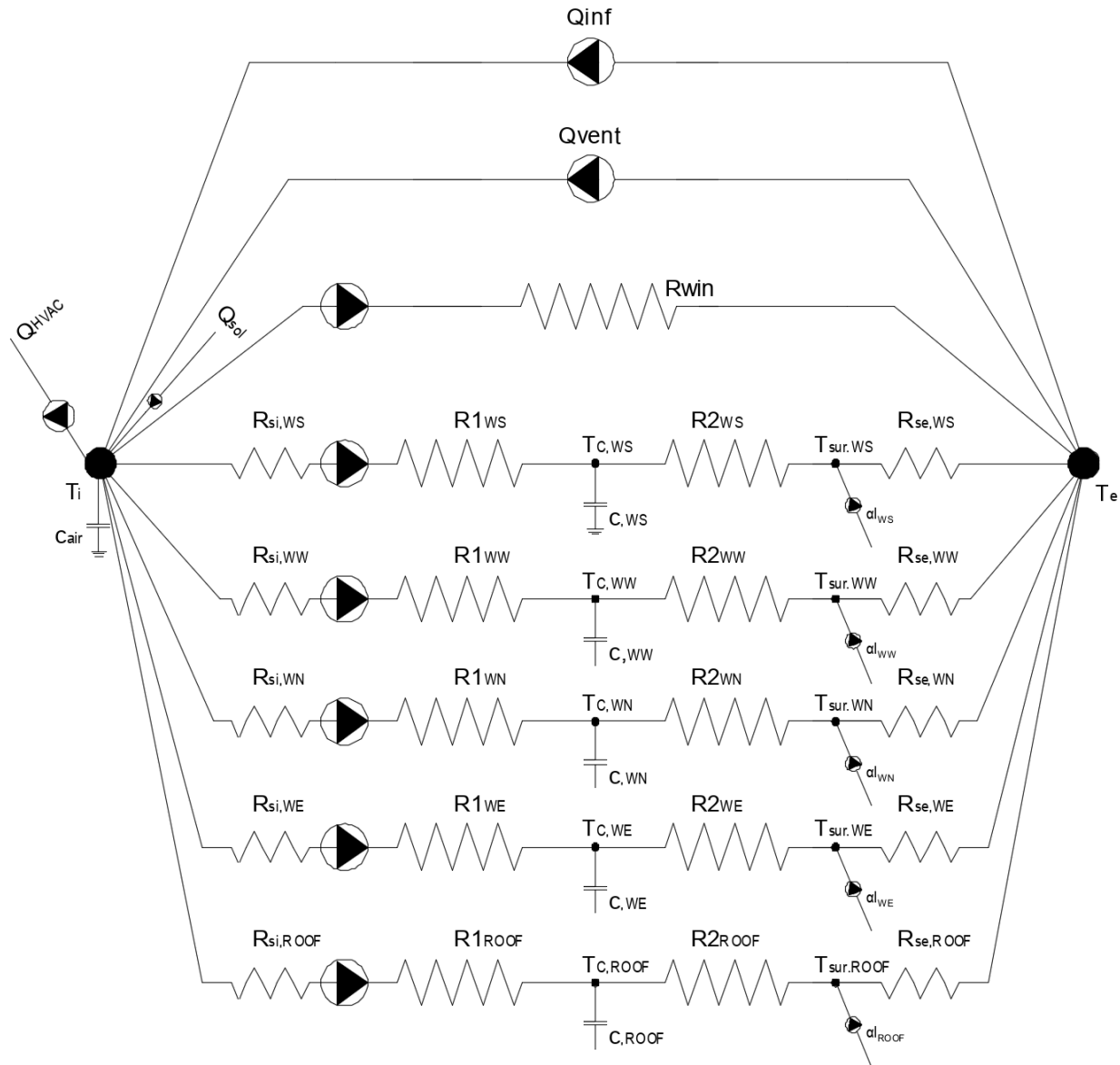


Figure 1 Equivalent circuit

Rather than the assumptions made for resistance and floor, some important factors that may affect the later result is tabulated, the highlighted in red represents high uncertainty whereas the blue one is of low uncertainty.

Table 1 Assumptions for the model

Assumptions
Internal gains are already included in the measured internal air temperature
Infiltration and ventilation rate keeps constant throughout the year
The location of thermal mass is fixed
Internal temperature at roof and floor are even, without stratification
No heat recovery in the mechanical system

3. Task 2

It is tasked to run the annual simulation to predict the heating and cooling loads for both lightweight and heavyweight buildings. The common and specific input for each case will be detailed to formulate a universal understanding. The results, consisting of the heating and cooling demand in hourly basis and weeks for the largest loads difference between two buildings, will be presented. A comparative analysis to discuss the differences between these two buildings is performed.

3.1. Input

The internal air temperature as a known parameter is collected from the HOBO in previous exercise. The data at 10/02/2018 was selected as the setpoint and repeated for the entire year. Provided that the data extracted from HOBO is recorded in every 10mins, first data of each hour will be used for the consistency of further analysis. In addition, both common and specific inputs for lightweight and heavyweight building are presented in “Lightweight_Integrated” and “Heavyweight_Integeated”.

3.2. Result

The heating and cooling loads in hourly basis are organised and presented in a sheet called “General results”. The hourly basis outcome could not either be tabulated or appended in this report owing to its substantial amount of data, it is probably more readable with heating, cooling and annual energy consumption for two buildings separately in Table 2.

Table 2 The simulation result

Heating energy (Wh/m ²)	Cooling energy (Wh/m ²)	Annual Energy consumption (Wh/m ²)
Lightweight building		
449159.3	-132650.7	581810.0
Heavyweight building		
410083.6	-144738.3	554821.9

Another output required is the selection of the weeks with highest differences in heating and cooling loads. The starting hour of each week is identified and labelled for fifty-two weeks which indicate the time interval of each week. Aided by the Excel functions, the spreadsheet can add heating or cooling loads data separately within the time interval previously labelled (“General result” sheet contains the selection procedures). By doing so, the hourly data is converted to weekly data for further comparison. The Table 3 summarises the processed data and shows that the greatest heating difference between lightweight and heavyweight building happens at week four, 80837.58W(h). Conversely, the cooling load at week fifty is very different for two buildings.

Table 3 Weeks with greatest difference

Week	Building type	Heating load (W)	Cooling load (W)	Difference (W)
Largest heating load difference				
4	Lightweight building	638929.22		80837.58
	Heavyweight building	558091.64		
Largest cooling load difference				
50	Lightweight building		-91550.32	33474.64
	Heavyweight building		-125024.96	

3.3. Discussion

Generally, it is observed that the annual energy consumption for heavyweight building is less than that of the lightweight building due primarily to the less requirement of heating demand. Given the temperate maritime climate in the UK, it is evident that it tends to be cool and often cloudy, driving the requirements of heating. Although both buildings have similar U value, heavyweight building employing the concrete block has much more capacity to store and release heat. This capability leads to a more even internal air temperature and thus less energy consumption. In terms of the heating difference at week four, this can be

similarly elucidated. The heavyweight with the effect of thermal mass has much better capability to store heat resulting in a steadier internal air temperature and less heating demand in the winter. On the contrary, the largest difference for cooling demand occurs at the fiftieth week. One hypothesis is that the dry bulb temperature increases sharply within a short time at that week. To verify this assumption, the external temperature, solar radiation and heat through walls for both building types at week fifty are compared. The data at 13/12/1983 is extracted that could potentially explain this phenomenon, more detailed data for the whole week can be obtained from the complementary file. Apparently, the hypothesis holds true considering the data provided in Table 4. Filled in red, the external temperature soared to 7.9°C from -5.3°C. The solar radiation, around 4000W, enters the room that is quite substantial compared with the solar radiation in the adjacent two days (~200W, shown in the supporting file). Additionally, it is observed that the heat flow through opaque elements at heavyweight building is considerably less than that of the lightweight building. Again, attributable to the thermal mass effect, the heavyweight building holds and stores the heat that will be released later when the outside temperature increased to 7.9°C. The accumulated heat requires much more cooling demand for heavyweight building to reach the setpoint, therefore the cooling load difference is substantial between two types of buildings.

Table 4 Verification of the hypothesis

Time and Temperature			Lightweigh building					Heavyweight building			
Date	HH:MM	Dry Bulb Temperature (C)	Qsolar (W)	Qws (W)	Qww (W)	QwN (W)	QwE (W)	Qws (W)	Qww (W)	QwN (W)	QwE (W)
13/12/1983	01:00	-3.0	0.0	137.6	232.2	309.6	232.2	41.6	70.3	93.8	70.3
13/12/1983	02:00	-3.1	0.0	137.2	231.6	308.8	231.6	42.2	71.4	95.2	71.4
13/12/1983	03:00	-3.9	0.0	138.6	233.9	311.9	233.9	43.1	72.9	97.2	72.9
13/12/1983	04:00	-4.2	0.0	140.9	237.8	317.1	237.8	44.0	74.4	99.2	74.4
13/12/1983	05:00	-4.8	0.0	143.0	241.3	321.7	241.3	44.4	75.1	100.2	75.1
13/12/1983	06:00	-4.7	0.0	144.8	244.4	325.9	244.4	45.1	76.2	101.7	76.2
13/12/1983	07:00	-5.6	0.0	147.1	248.2	331.0	248.2	46.0	77.7	103.7	77.7
13/12/1983	08:00	-5.3	0.0	148.7	251.0	334.6	251.0	46.4	78.4	104.6	78.4
13/12/1983	09:00	-3.6	94.7	146.4	247.1	329.5	247.1	46.6	78.8	105.1	78.8
13/12/1983	10:00	-2.5	735.9	140.9	240.3	320.4	238.2	49.2	83.2	110.9	83.1
13/12/1983	11:00	-0.2	2149.3	121.5	221.0	294.6	211.6	46.0	78.7	104.9	78.1
13/12/1983	12:00	6.2	4033.4	86.1	191.5	255.4	174.5	41.7	73.4	97.9	72.2
13/12/1983	13:00	7.9	3207.5	54.1	159.1	212.4	145.1	37.2	68.0	90.7	66.6
13/12/1983	14:00	7.3	414.2	53.6	141.5	189.2	135.4	34.0	63.3	84.5	62.0
13/12/1983	15:00	7.1	198.8	67.1	136.7	182.6	134.0	31.9	59.2	79.0	58.1
13/12/1983	16:00	6.9	37.9	75.7	138.4	184.7	137.2	30.8	56.8	75.8	55.7
13/12/1983	17:00	6.9	0.0	80.3	140.4	187.3	139.8	29.6	54.3	72.5	53.4
13/12/1983	18:00	6.9	0.0	82.5	141.5	188.7	141.2	28.7	52.4	69.9	51.6
13/12/1983	19:00	7.1	0.0	83.1	141.2	188.3	141.1	27.9	50.7	67.6	49.9
13/12/1983	20:00	7.2	0.0	82.7	140.1	186.8	140.0	27.1	49.0	65.4	48.3
13/12/1983	21:00	7.3	0.0	82.3	139.1	185.5	139.1	26.6	47.9	63.9	47.2
13/12/1983	22:00	7.2	0.0	82.2	138.8	185.1	138.8	26.4	47.2	63.0	46.6
13/12/1983	23:00	7.2	0.0	78.1	131.9	175.9	131.9	21.6	39.0	52.0	38.4
13/12/1983	24:00:00	7.1	0.0	80.6	136.0	181.3	136.0	23.4	41.7	55.6	41.2

4. Task 3

Sensitivity analysis normally splits into two analysis categories, local and global analysis. In this report, mainly the Monte Carlo analysis is performed that considers the interactions between variables, yielding more accurate result (Tian, 2013). However, the temperature effect due to the climate change is analysed using local or differential sensitivity analysis, owing to the fact that the temperature for each year is obtained from weather file instead of statistical distributions. The results being discussed is the energy consumption in preference to heating and cooling loads of the selected weeks. This is because controlling one output tends to produce more consistent comparison result.

Parameters that potentially imposes a great influence on the energy consumption for lightweight building are exhibited in Table 5. The statistical distributions are assigned with corresponded characteristics values (mean and standard deviation). However, the selection of distribution types could greatly influence the final result and requires more studies. Aided by excel Data Table analysis, a thousand data within the assigned distribution range is generated for each parameter.

Table 5 Key parameters for sensitivity analysis

Assumption						
Parameters	Sub-parameters	Distribution	p1	p2	Random variables within the distribution	
Orientation		Uniform	-45.0000	45.0000	27.3321	
Material properties	Wall_Thermal conductivity_Fiberglass quilt	Normal	0.0500	0.0200	0.0653	
	Wall_Thickness_Fiberglass quilt	Normal	0.0700	0.0400	0.0969	
Surface properties	Wall_Thermal absorptance (emissivity)	Normal	0.5000	0.1500	0.5504	
	Window_Solar absorptance	Normal	0.6500	0.1500	0.5844	

The results are plotted and shown in following figures.

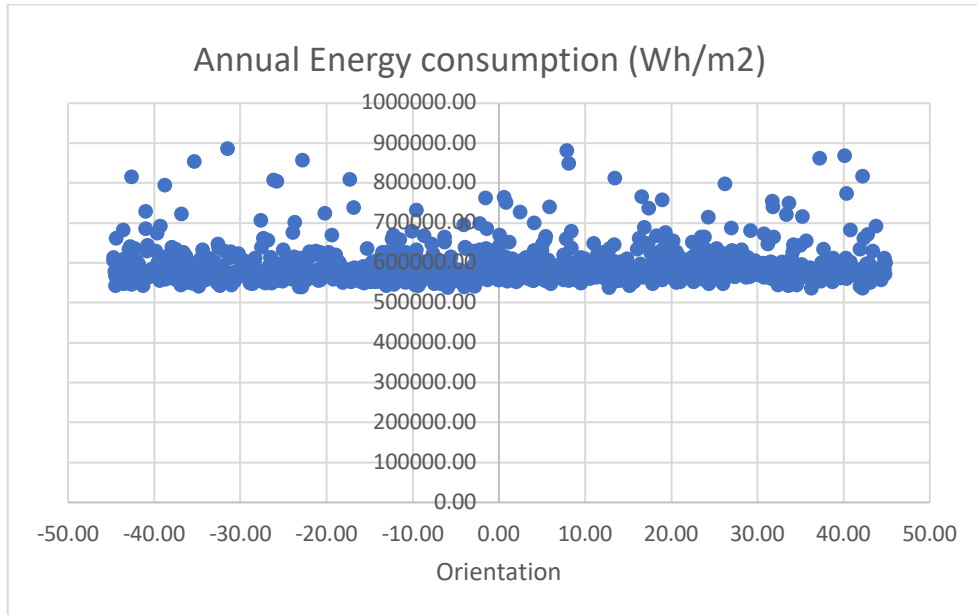


Figure 2 Sensitivity of orientation

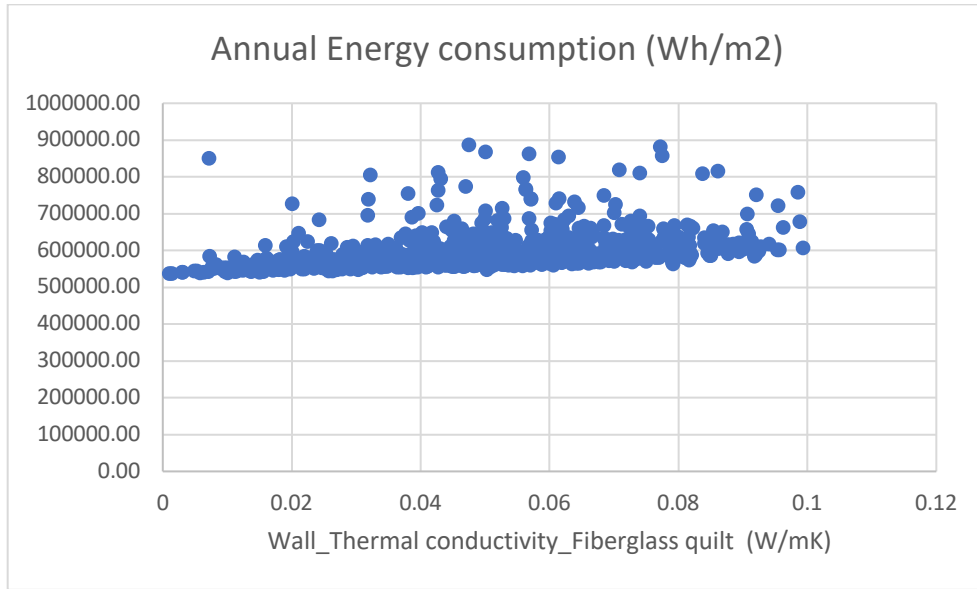


Figure 3 Sensitivity of thermal conductivity

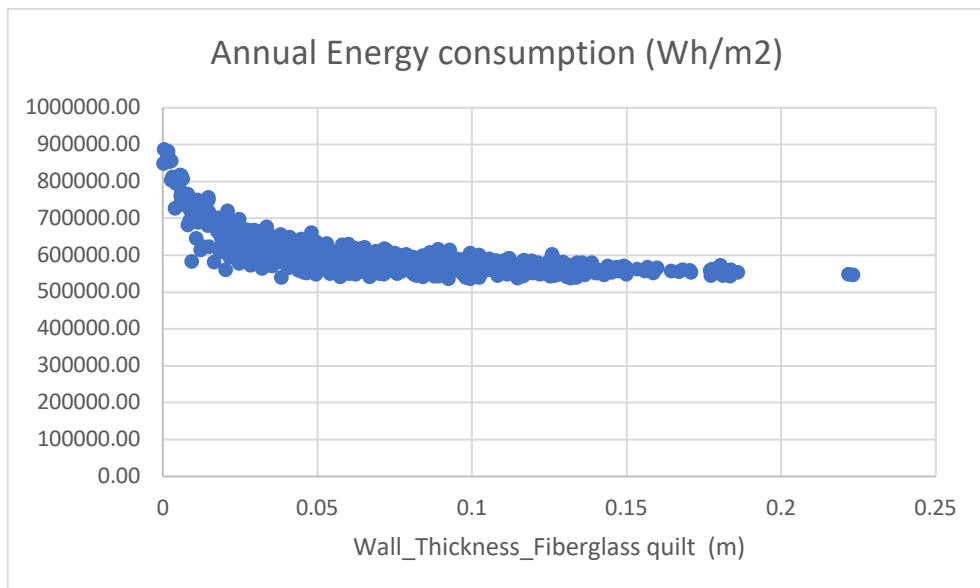


Figure 4 Sensitivity of insulation thickness

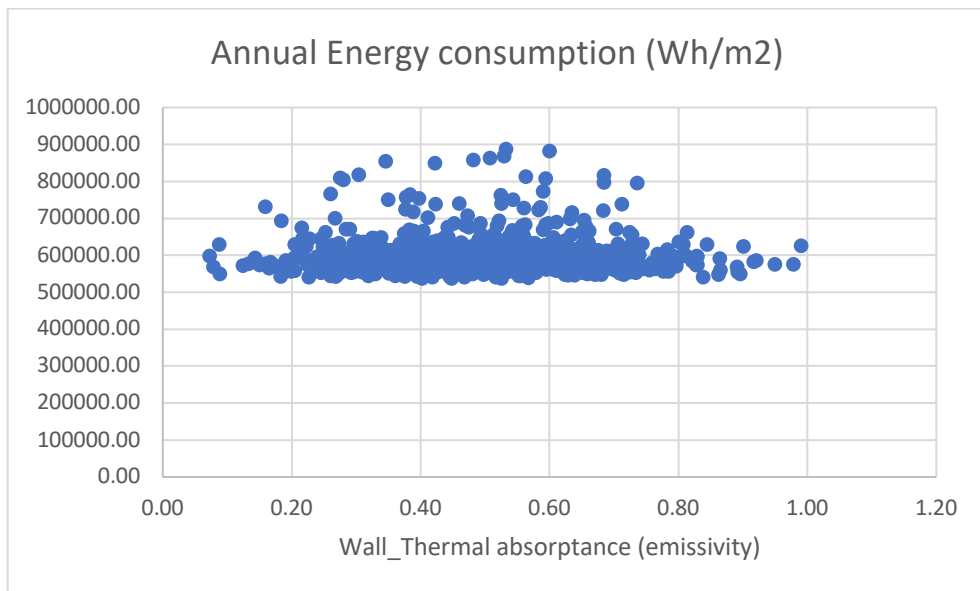


Figure 5 Sensitivity of wall absorptance

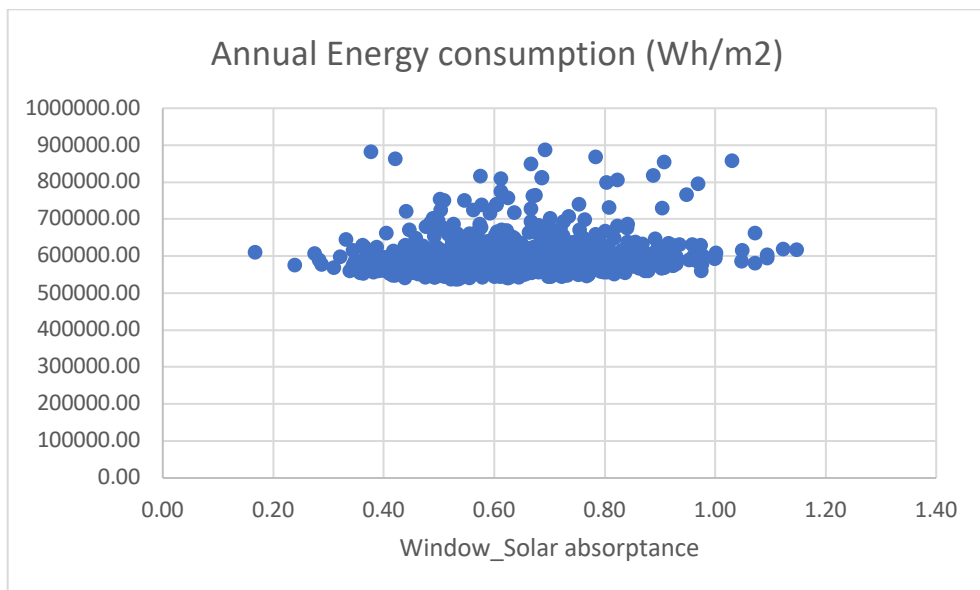


Figure 6 Sensitivity of solar absorptance

It is difficult to visually describe the scatter plots. Statistical tests are used to quantify the relationships between sensitive parameters and annual energy consumption. Pearson and Spearman coefficients, assuming linear and non-linear relationship, are used and the results are shown in Table 6 (Symonds, 2018).

Table 6 Sensitivity result

	Spear	Rank	SSpear	Rank
Orientation	0.0288	4	0.0547	4
K (W/mK)	0.3720	2	0.5496	2
d (m)	-0.6677	1	-0.7497	1
α	-0.0280	5	-0.0171	5
g	0.0873	3	0.1401	3

Both correction coefficients confirm that, the thickness of fibreglass quilt is the dominating factor, followed by the thermal conductivity. The wall absorptivity has the least influence on the total energy consumption.

The future temperature files accounting for the climate change are used to perform a local sensitivity analysis. The result is displayed in Table 7. The annual consumption is reduced, partly because UK tends to be cold throughout a year. The global warming effect increases the outside dry bulb temperature which possibly leads to smaller gap with indoor setpoint, hence the heating demand is reduced. Cooling is increased but not as much as heating, leading to total energy consumption reduction. The temperature effect is marginally sensitive compared with the parameters shown above, however this result is limited by the sample size. More information could be found at sheet “Lightweight_SA” and “SA_Monte Carlo Generator_Lightweight” (Tips: the generator file requires high memory).

Table 7 Sensitivity of climate change

Future Weather_data	Heating energy (Wh/m2)	Cooling energy (Wh/m2)	Annual Energy Consumption (Wh/m2)	ΔY
GBR_London.Gatwick.037760_IWECE	449159.3455	-132650.6912	581810.0368	Base case
2030_Islington_a1b_10_percentile_TRY	424676.8453	-145746.5473	570423.3926	-11386.644
2030_Islington_a1b_33_percentile_TRY	408388.0003	-156100.2025	564488.2028	-17321.834
2030_Islington_a1b_50_percentile_TRY	399935.2826	-161812.248	561747.5306	-20062.506
2030_Islington_a1b_66_percentile_TRY	392114.6806	-167574.4715	559689.1521	-22120.885
2030_Islington_a1b_90_percentile_TRY	371215.1052	-182168.428	553383.5332	-28426.504
2050_Islington_a1b_10_percentile_TRY	414172.5434	-152911.2593	567083.8027	-14726.234
2050_Islington_a1b_33_percentile_TRY	394976.628	-163074.0279	558050.6559	-23759.381
2050_Islington_a1b_50_percentile_TRY	386474.989	-171282.9473	557757.9362	-24052.101
2050_Islington_a1b_66_percentile_TRY	375916.3911	-178720.8121	554637.2032	-27172.834
2050_Islington_a1b_90_percentile_TRY	353646.4909	-196745.6402	550392.1311	-31417.906
2080_Islington_a1b_10_percentile_TRY	403834.1242	-157882.5633	561716.6875	-20093.349
2080_Islington_a1b_33_percentile_TRY	382425.2922	-174959.8623	557385.1545	-24424.882
2080_Islington_a1b_50_percentile_TRY	369241.2717	-185594.7532	554836.0249	-26974.012
2080_Islington_a1b_66_percentile_TRY	355315.0433	-194742.4404	550057.4837	-31752.553
2080_Islington_a1b_90_percentile_TRY	327262.8196	-217330.79	544593.6096	-37216.427

5. Conclusion

Task 1 rearranged the equation provided by Gori and forms a complete system to calculate the energy demand to reach the setpoint. The assumptions are presented which may result in large uncertainties. For instance, the constant ventilation rate is unlikely to happen in practice due to for example, workmanship, wind or the stack effect. Further work is recommended to investigate the uncertainties which could be integrated into Gori’s method for better accuracy. The second task indicates that the heavyweight building is more energy efficient over lightweight building at the same comfort level in the UK. This fact is not applicable to other locations as the thermal storage is highly dependent on the climate. Additionally, it is commonly agreed that the thermal mass effect should be used coupling with night cooling or great finishes. These factors are ignored but requires great care to generate a more realistic energy consumption in the future. The sensitivity analysis result is greatly influenced by the quality of inputs, the selection of better distribution types is recommended for future analysis by referring to the insitu data or literatures. The number of parameters selected to perform the sensitivity analysis could be expanded. The sampling size is also significant that compromise the accuracy of result. Apart from sensitivity of each parameter, some interesting findings worth mentioning, for instance the thickness of fibreglass quilt is only crucial when it is less than 0.05m. This result can inform designer to produce a cost-effective approach to build the building.

6. References

GORI, V. (2017) A NOVEL METHOD FOR THE ESTIMATION OF THERMOPHYSICAL PROPERTIES OF WALLS FROM SHORT AND SEASONALLY INDEPENDENT IN-SITU SURVEYS. UNIVERSITY COLLEGE LONDON.

Symonds, P. (2018) 'Lecture Notes: Sensitivity and Uncertainty Analysis'. London, pp. 43–54.

Tian, W. (2013) 'A review of sensitivity analysis methods in building energy analysis', Renewable and Sustainable Energy Reviews. doi: 10.1016/j.rser.2012.12.014.